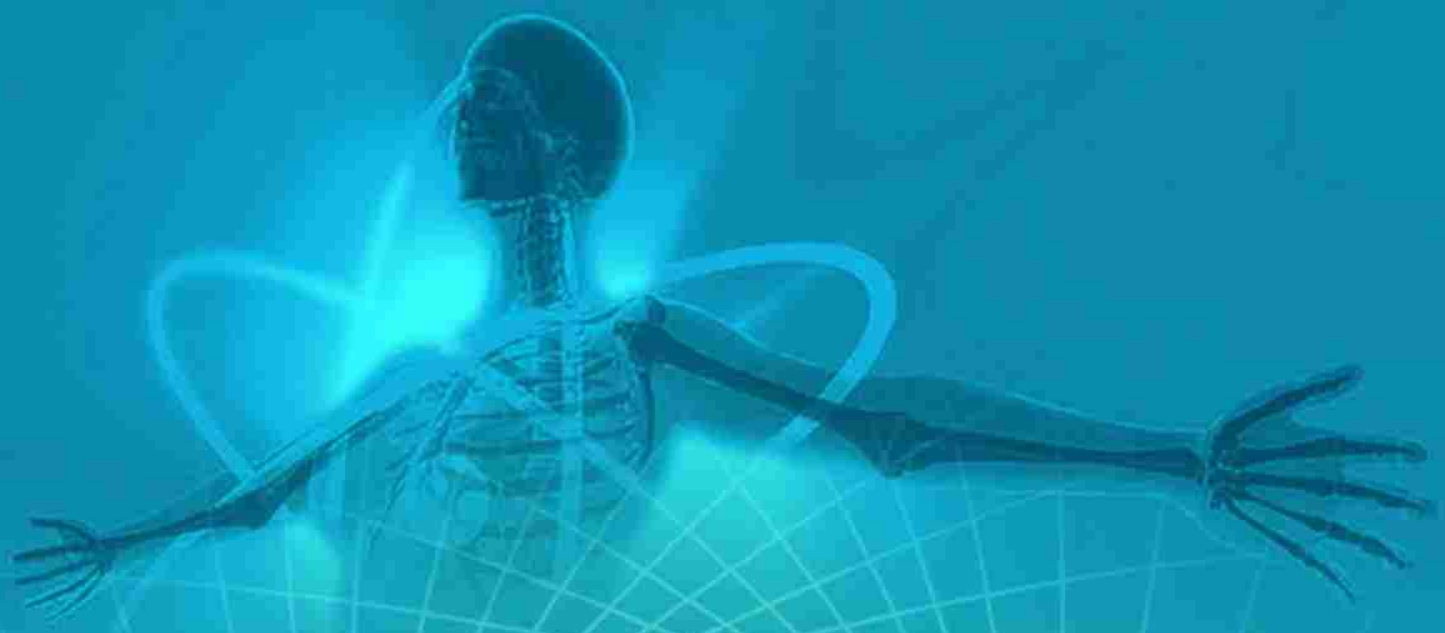

چکیده مقالات سخنرانی

بیست و چهارمین همایش سالیانه
انجمن علمی پزشکی هسته‌ای ایران

۶ تا ۸ دی‌ماه ۱۴۰۲

به نام خداوند لوح و قلم حقیقت نگار وجود و عدم

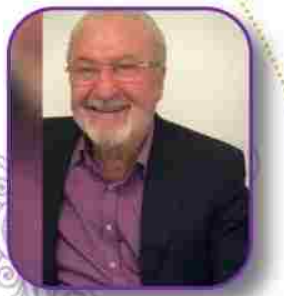

دکتر محسن ساغری

استاد دانشگاه علوم پزشکی تهران

عضو پیوسته فرهنگستان علوم پزشکی ایران

حرفه پزشکی در اسلام مقدس می باشد، یک پزشک باید توجه داشته باشد که خداوند متعال او را برای چنین مسئولیتی انتخاب نموده و ناظر به تمام اعمال و رفتار اوست و در واقع تجلی اسم شافی پروردگار است که در عالم ملک ظهور پیدا کرده ا ست و با چنین باوری باید جایگاه خود را بهتر بشناسد. اصول اخلاقی مندرج در متون پزشکی کهن دوران تمدن اسلام و ایران شامل نرم خوئی، خوش رفتاری، مهربانی، دلسوزی، رفتار انسانی، اخلاقی، عاطفی و صمیمانه، شرافت مندانه و احترام آمیز همراه با حفظ اسرار بیمار، خردمندی و با سواد بودن پزشک، رعایت تقوا، توکل و توسل همیشگی او به درگاه ایزدمنان در حل مشکلات و پرهیز از هر گونه اهانت به همکاران باشد از آنجا که رشته پزشکی هسته ای به دلیل وسعت، پیچیدگی و ظر افت های خاص آن نیازمند بهره گیری از دانش و تجربه متخصصان مختلف در این زمینه می باشد، اخلاق حرفه ای در پزشکی هسته ای در چهار چوب عملکرد هر یک از این متخصصان است رعایت اخلاق حرفه ای موجب بهره وری بیشتر بیماران و رضایت آنها، رضایت پزشکان ارجاع دهنده، توسعه خدمات پزشکی، رضایت خاطر ارائه دهنده گان خدمت و همچنین جلوگیری از قصور و پیامد های ناشی از آن و در نهایت کمک به بهبود و توسعه نظام سلامت خواهدگردید.

Oral Presentation Papers

Intra-operative lymphatic mapping and sentinel node biopsy in laryngeal carcinoma using radiotracer injection

Pegah Sahafi; Amin Saber Tanha; Maryam Daghighi; Ehsan Khadivi; Kamran Khazaeni; Vahid Reza Dabbagh Kakhki; Ramin Sadeghi

Introduction: The purpose of this study was to determine the value of sentinel lymph node biopsy in the laryngeal SCC, using intra-operative peri-tumoral injection of Tc-99m-phytate.
Material and methods: Patients with biopsy-proven squamous cell carcinoma of the larynx were included. On the day of surgery, after anesthesia induction, suspension laryngoscopy was performed to inject 2mCi/0.4 cc Tc-99m-phytate in four aliquots into the sub-mucosal peri-tumoral location. After 10-minute wait, portable gamma probe was used to locate sentinel nodes. Subsequently, all patients underwent laryngectomy and neck dissection. Both sentinel nodes and non-sentinel nodes were examined using hematoxylin and eosin (H&E) staining.
Results: Twenty-six patients with diagnosis of laryngeal carcinoma were included in the study. The sentinel lymph node (SLN) detection rate was 65.4% (17 out of 26; 1.31 sentinel nodes per patient), with 100% detection rate in the supraglottic region (7 out of 7) and 52.6% detection rate for glottis/transglottic patients (10 out of 19). Permanent pathology results showed lymph node involvement in four patients, but only one patient had positive result in the sentinel lymph node biopsy (SLNB), resulting in an overall false negative rate of 25%. The sensitivity of the SLN technique was 75% overall, 100% in the supraglottic region, and 67% in the glottis/transglottic region.
Conclusion: Accuracy and feasibility of sentinel lymph node biopsy may be related to the location of the tumor in the larynx. For supraglottic tumors, the technique seems to be feasible with low false negative rate. For glottis/transglottic tumors both detection rate and false negative rate seem to be suboptimal. Further studies are needed to validate our results.

Oral Presentation Papers

Diagnostic value of multiphasic ^{68}Ga–PSMA-11 PET/CT imaging in detection of prostate bed recurrence and regional lymph node metastasis in prostate cancer patients

Zahra Bakhshi[1], Atena Aghaee[1], Vahid Roshanravan[1], Habibollah Dadgar[2], Emran Askari[1], Kamran Aryana[1], Nasim Norouzbeigi[2], Susan Shafiei;

1. Nuclear Medicine Research Center, Mashhad University of Medical Sciences, Mashhad, Khorasan Razavi, Iran
2. Razavi Cancer Research Center, Razavi Hospital, Imam Reza International University, Mashhad, Iran

Background: A way to improve the accuracy of ^{68}Ga-PSMA-11 PET/CT scans is to perform multiphasic acquisitions. The aim of this study is to evaluate the clinical utility of early and delayed imaging in prostate cancer (PCa) patients as well as temporal changes in the semi-quantitative parameters.

Material and Methods: In this single-center retrospective study, 138 PCa patients were referred for ^{68}Ga-PSMA PET/CT scan for various indications. Patients underwent standard 60 min imaging along with the first 4-min post-injection static acquisition, and delayed imaging, 2.5-3 h after injection, both from the pelvic field. Changes in the lesion SUVmax and target-to-background ratios (TBR) were recorded for each phase of the imaging.

Results: The positivity rates for PSMA-avid lesions in the early, whole-body, and delayed images were 71.5% (93/130), 73.9% (77/110), and 70% (77/110), respectively. In the early, total, and delayed phases, the total number of PSMA-avid lesions were 305, 340, and 239, respectively. The most prevalent lesions were found in the prostate gland or bed, lymphatic stations, and bone. The median SUVmax values for local recurrence, lymph nodes, and bone were 9.14, 7.36, and 4.83 in the early phase, 13.89, 15.78, and 11 in the whole-body phase, and 13.13, 19.19, and 7.78 in the delayed phase, respectively. The detection rates for local recurrence in the early, whole-body, and delayed phases were 13.8% (18/130), 15.9% (22/138), and 17.3% (19/110), respectively, with no statistically significant change (p=0.5). The detection rates for lymph node metastases were

23.8% (31/130), 29% (40/138), and 28% (30/110), with a significant difference observed between the early and whole-body phases (p=0.016). The detection rates for osseous lesions in the early, whole-body, and delayed images were 28.46% (37/130), 27.53% (38/138), and 21.81% (24/110), respectively, with no statistically significant difference found (p=0.139).

Conclusion: The detection rates of bone lesions were comparable across all three phases. The early phase imaging was more effective for evaluation of local bladder invasion but was less successful in identifying prostate bed lesions, seminal vesicle invasion, and lymph node metastases. The increased SUVmax pattern appeared more prominent in corrected SUVmax (T/BG) than in SUVmax for various lesions. Additionally, the increasing pattern of SUVmean demonstrated a smaller increase in the proportion of patients compared to SUVmax in the transition from early to whole-body and early to delayed phase images.

Keywords: [^{68}Ga]Ga-PSMA-11 PET/CT scan, prostate cancer, early phase, whole-body phase, delayed phase.

Oral Presentation Papers

^{68}Ga-FAPI-46 PET/CT in a metastatic castration-resistant prostate cancer patient

Soroush Zarehparvar Moghadam [1], MD; Reyhaneh Manafi-Farid[2], MD; Hamidreza Amini[3], MD; Ghasemali Divband[3], MD; Kamran Aryana[4], MD

1. Nuclear Medicine Research Center, Mashhad University of Medical Sciences, Mashhad, Iran
2. Research Center for Nuclear Medicine, Shariati Hospital, Tehran University of Medical Sciences, Tehran, Iran
3. Khatam PET/CT center, Khatam-al-anbia hospital, Tehran, Iran

Background: In metastatic castration resistant prostate cancer (mCRPC) patients, prostate specific membrane antigen (PSMA) expression is heterogenous and around 10% of prostate cancers do not express PSMA. Fibroblast activation protein is overexpressed in many cancers including prostate cancer. Ga-FAPI-46 PET/CT may be an alternative imaging method in patients with low or absent PSMA expression.

Material and Methods: A 70 years-old man with mCRPC was referred for ^{68}Ga-PSMA PET/CT for evaluation of PSMA expression status and possibility of PSMA-targeted radioligand therapy.

Results: ^{68}Ga-PSMA PET/CT showed numerous PSMA-positive skeletal metastases however the SUVmax of lesions were low (Figure 1a and 1b). Considering the low PSMA expression, ^{68}Ga-FAPI-46 PET/CT was requested to evaluate FAP expression and eligibility for ^{177}Lu-FAPI therapy. ^{68}Ga-FAPI PET/CT also showed numerous skeletal metastases with SUVmax relatively higher than PSMA PET/CT (Figure 1c and 1d). However; as comparing two PET scans heterogeneous uptake was noted between two tracers. For example, the uptake of the lesions in the sternum was lower in PSMA PET than in FAPI PET, although the pelvic lesions showed higher uptake in the PSMA PET. Overall, the uptake of the both tracers were not significantly different form each other and the patient received two doses of ^{177}Lu-PSMA. A partial biochemical response was observed however the bone pain was not alleviated and the patient ceased one months after the second course of radioligand therapy.

Conclusion: Usually mCRPC patients experienced multiple lines of treat-

ment before receiving radioligand therapy and as a result the disease become more resistant to therapies. Also in mCRPC patients with low or absent PSMA expression, FAPI theranostics may play a role in managing mCRPC patients whom are resistant to other treatments.

Oral Presentation Papers

3D Monte Carlo patient specific dosimetry in 177Lu-PSMA therapy of mCRPC patients

Sirwan Maroufpour[1], Kamran Aryana[2], Shahrokh Nasseri[1], Zahra Fazeli[2], Hossein Arabi[3] ,Mehdi Momennezhad[1]

1. Medical Physics Group, Faculty of Medicine, Mashhad University of Medcal Sciences, Mashhad, Iran
2. Nuclear Medicine Research Center, Faculty of Medicine, Imam Reza Hospital, Mashhad University of Medical Sciences, Mashhad, Iran.
3. Division of Nuclear Medicine and Molecular Imaging, Geneva University Hospital, CH-1211 Geneva 4, Switzerland

Introduction: Prostate cancer is the second most common cancer worldwide and the fifth leading cause of cancer-related death in men. In the treatment of these patients, various methods are used, including the use of radiopharmaceutical 177Lu-PSM A-617 in the treatment of metastatic castration-resistant prostate cancer (mCRPC) patients. In recent years, there are several studies on application of this radiopharmaceutical in various fields such as response to treatment, the amount of prescription activity, internal dosimetry and the identification of critical organs. The aim of this study was to investigate the internal dosimetry of patients treated with 177Lu-PSM A-617 in the nuclear medicine department of Ghaem Hospital.

Material and Methods: In this study, the absorbed dose of different organs of 9 mCRPC patients in the first cycle of treatment was investigated. Whole body planar and and SPECT / CT images were taken in 1 ± 0.5, 4 ± 0.5, 24 ± 2, 48 ± 2, 72 ± 2 and 144 ± 2 hours after administration. The Q-MATRIX software was used for reconstruction and 3D-SLICER was used for quantification and segmentation. In this study, the absorbed dose of organs and metastases were calculated using the Monte Carlo Gate code version 8.

Results & Discussion: The mean absorbed doses of organs calculated by Gate for first cycle were (0.36 Gy / GBq) for Kidneys, (0.09 Gy/GBq) for Liver, (0.51 Gy / GBq) for Submandibulars Glands, (0.56 Gy / GBq) for Parotid Glands, (2.81 Gy / GBq) for Lacrimal Glands and (3.91Gy / GBq) for Metastasis.

Conclusion: The absorbed dose of organs in the first cycle of treatment was less than the tolerable limits. however, for the administered dose in the next

cycles of treatment, the total cumulative absorbed dose should be considered.

Oral Presentation Papers

Non-malignant 68Ga-FAPI-46 uptake in two cases of TENIS syndrome:- comparison with 18F-FDG

Farivash Karamian[1], Ramin Sadeghi[1], Emran Askari[1], Atena Aghaee[1], Hessamodin Rostaei[1]

1. Nuclear Medicine Research Center, Mashhad University of Medical Sciences, Mashhad, Iran.

Introduction: TENIS syndrome, characterized by elevated thyroglobulin levels and negative iodine scintigraphy, poses a diagnostic challenge in thyroid cancer management. While ^{18}F-FDG PET/CT has traditionally been the standard imaging modality for assessing TENIS syndrome, recent studies have shown promising results with ^{68}Ga-FAPI PET/CT. This novel imaging technique targets fibroblast activation protein and has emerged as a potential alternative for these cases. However, it is important to understand the potential pitfalls and limitations of ^{68}Ga-FAPI PET/CT. This case report aims to highlight some of these pitfalls and challenges, comparing the findings with concurrent FDG PET/CT.
Methods: Two middle-aged women with a history of TENIS syndrome and high serum thyroglobulin levels underwent both ^{68}Ga-FAPI-46 PET/CT and ^{18}F-FDG PET/CT scans to search for possible metastasis sites.
Results: Neither the ^{68}Ga-FAPI PET/CT nor the ^{18}F-FDG PET/CT scans revealed any suspicious tumoral involvement. However, a few non-malignant uptakes were observed on the FAPI study. The atrophic parotid gland exhibited FAPI uptake, which was not consistent with the FDG scan. This finding correlated with chronic parotiditis observed on the CT images. Additionally, increased uptake was observed in the gallbladder on the FAPI scan, while no uptake or pathological findings were seen on the FDG or CT images. Intense uptake in the FAPI scan and moderate FDG uptake were observed in the degenerative changes of the L5-S1 facet joint, with sclerotic changes visible on the CT images. The uterus demonstrated intense uptake in the FAPI scan, while only mild uptake was seen in the FDG, and no underlying pathology was evident on the CT images. It is important to note that this post-menopausal woman had no history of gynecological disease.
Conclusion: Fibroblast activation protein inhibitor (FAPI)-targeted radio-

pharmaceuticals are being explored as potential alternatives to FDG for tumor-specific imaging. However, it has been observed that these radiopharmaceuticals can also accumulate in benign diseases and normal tissues. This is due to the expression of fibroblast activation protein (FAP) during various physiological processes such as embryogenesis, wound healing, inflammation, and fibrosis. Therefore, when interpreting a FAPI study, it is crucial to consider non-malignant causes of FAPI uptake.

Keyword: TENIS syndrome, FDG, FAPI, PET/CT, Thyroglobulin, Pitfall

Oral Presentation Papers

Prediction of Gleason score of prostate cancer using machine learning model in 68Ga-PSMA PET/CT images

Zahra Vosoughi[1], Sahar Faraji[2], Habibeh Vosoughi[3], Farshad Emami[4]

1. Department of Medical Physics, School of Medicine, Shahid Sadoughi University of Medical Sciences, Yazd, Iran.
2. Department of Medical Physics, Mashhad University of Medical Science, Mashhad, Iran.
3. Research Center for Nuclear Medicine, Shariati Hospital, Tehran University of Medical Science, Tehran, Iran.
4. Nuclear Medicine Department, Razavi Hospital, Imam Reza International University, Mashhad, Iran.

Introduction: The aim of this study is the evaluation of different machine learning algorithms to predict Gleason Score (GS) in primary prostate cancer (PCa) using radiomics features of 68Ga-PSMA PET/CT images.
Materials and Methods: 128 cases with PCa referred to the nuclear medicine department who underwent 68Ga-PSMA-PET/CT for staging before giving any medical treatment, were enrolled. All patients are grouped based on GS (group 1: GS=7, group 2: GS=8 and group 3: GS=9). The tumor in the prostate bed was diagnosed and segmented from 68Ga-PSMA-PET/CT images by an experienced nuclear medicine physician. Radiomics features including shape, first-order, GLCM, GLRLM, GLSZM, and GLDM were extracted from the volume of interest (VOI) of segmented tumor PET and CT images. After that, 8 features are selected by Recursive Feature Elimination (RFE). Seven models were assessed, including support vector machine (SVM), Logistic regression (LR), Random Forest (RF), Decision Tree (DT), Gradient Boosting Classifier (GBC), MLP Classifier and K-neighbors. Models were trained by PET-only, CT-only and PET/CT features were generated by combining features at the feature level, separately. The performance of all models was evaluated based on the area under the curve (AUC).
Result: All seven models that were applied to predict GS were compared to each other using AUC. Four models had higher predictive performance among all models trained by CT features. Firstly, the best predictive per-

formance for GS=7 was reached by LR and MLP where AUC for LR were 0.74. Also for MLP Classifier same result was reached. Secondly, for GS=8, SVM achieved the best results, in which AUC. Then, for PCa patients with GS=9, RF reached the best predictive performance on CT images, achieving an AUC of 0.75. The results indicate that all models had the lowest predictive performance on PET images. Finally, LR recorded the best predictive performance on PET/CT images with AUC 0.77 for GS=7, AUC 0.73 and AUC 0.77 for GS=8 and GS=9, respectively.

Conclusion: The results of this study show that radiomics models based on CT images and combining features could be a non-invasive method to predict pathological GS (GS=7, GS=8 and GS=9) in primary PCa.

Keywords: Prostate Cancer, 68Ga-PSMA PET/CT, Radiomics, Machine Learning, Gleason Score.

Oral Presentation Papers

Deep Learning for Classification of Dual-Energy X-ray Absorptiometry of Postmenopausal Women

Hojjat Mahani[1*], Elaheh Tarighati[2]

1. Radiation Applications Research School, Nuclear Science and Technology Research Institute, P.O. BOX: 14395-836, Tehran, Iran
2. Department of Medical Physics, Iran University of Medical Sciences, Tehran, Iran

Background and Objectives: Bone mineral density (BMD) scans play a vital role in the early diagnosis and treatment of osteoporosis, particularly for postmenopausal women. Dual-energy X-ray absorptiometry (DXA) is a well-established imaging modality for such tasks. The T-score is a DXA measure representing the difference between the patient's BMD and the average BMD of young/healthy adults of the same sex. Therefore, this work aims to classify a DXA scan into (1) normal, (2) osteopenia, and (3) osteoporosis classes using deep learning. **Materials and Methods:** To do so, DXA scans (femoral neck and/or lumbar vertebrae) of 210 postmenopausal women were acquired. The vendor-provided DXA test reports were considered as ground truth. The dataset portioning into training, validation, and test sets was 5:1:1. A pre-trained convolutional neural network was then exploited to classify the DXA scans. The performance of the deep classifier was evaluated in terms of sensitivity, specificity, and the area under the receiver operating characteristics curve (ROC AUC). **Results:** The results show an encouraging performance of the utilized deep classifier. The findings are comparable to those of the DXA test reports by offering a sensitivity of 0.91 and a specificity of 0.87. The calculated ROC AUC is 0.89 indicating the promising performance of the exploited multiclass deep neural network in the classification of the DXA scans. An accuracy of higher than 0.93 is also observed. **Conclusion:** The findings demonstrate fast and accurate classification of DXA scans into (1) normal, (2) osteopenia, and (3) osteoporosis classes. By exploiting the proposed architecture, the risk of fractures can be significantly reduced for postmenopausal women.

Keywords: DXA scan; Postmenopausal women; Deep learning; Osteoporosis

Oral Presentation Papers

TB-GAN: A new developed Deep Learning Framework for SPECT Myocardial Perfusion Image Denoising

Seyed Mohammad Entezarmahdi[1,2], Amin Karimi[1], Fatemeh Dehghan[2], Reza Faghihi

1. Nuclear Engineering Department, Shiraz University, Shiraz, Iran
2. Nuclear Medicine Department, School of Medicine, Shiraz University of Medical Sciences, Shiraz, Iran

Introduction: In the field of single-photon emission computed tomography (SPECT) myocardial perfusion imaging (MPI), image denoising is a critical issue as it can impact clinical decision. This paper introduces an innovative deep neural network approach aimed at improving the quality of SPECT myocardial perfusion images by minimizing noise.

Methods: This study was conducted on 407 individuals using a dual head gamma camera. Myocardial perfusion SPECT was performed with a projection time of 26 seconds to acquire images with standard noise levels. Immediately following the SPECT imaging, a 180-second planar scan was initiated (anterior and lateral views). This latter scan served as the high-quality, low-noise ground truth.

The deep network structure proposed in this study, referred to as TB-GAN (Two-branches generative adversarial network), is composed of two encoder paths and one decoder section. One encoder network is responsible for computing the noise features, while the other extracts the signal features. The output features from these two encoders are combined and fed into a decoder to reconstruct a low-noise image. A discriminator network is employed as the adversarial objective function.

The results obtained from this method were compared with those from the traditional noise-to-clean U-Net GAN framework. Quantitative evaluation was carried out using the peak signal-to-noise ratio (PSNR), structural similarity index (SSIM), and root mean square error (RMSE).

Results: The quantitative assessment revealed a statistically significant enhancement in both PSNR and SSIM when utilizing the proposed framework. Specifically, PSNR increased from 34.74 to 41.95 and SSIM

from 0.805 to 0.949 when comparing TB-GAN to the traditional GAN. Although the traditional GAN network produced outputs with a slightly lower RMSE than TB-GAN, the difference was not statistically significant (RMSE=0.116 for GAN vs. 0.159 for MV-GAN). Furthermore, both visual and count profile analyses demonstrated the superior performance of the proposed network.

Conclusion: The newly proposed deep neural network structure named as TB-GAN, designed for enhancing image quality in SPECT myocardial perfusion images, has demonstrated superior noise reduction results compared to the traditional noise-to-clean U-Net GAN framework.

Keywords: Myocardial Perfusion Imaging, Deep Neural Network, Image Denoising

Oral Presentation Papers

"Investigating the role of F18-FDG PET/CT and Ga68 DOTATOC PET/CT in the evaluation of differentiated thyroid cancer patients with increased serum thyroglobulin and negative I-131 whole body scan"

Atena Aghaee, MD, Kamran Aryana, MD; Mohammad Esmatinia, MD; Seyed Rasoul Zakavi, MD; Susan Shafiei, MD

Objective: Regarding increasing prevalence and incidence of thyroid cancer on a global and regional scale, and considering majority of thyroid cancer is consisted of differentiated thyroid cancer, as well as facing challenges in managing cases with elevated Tg negative whole body iodine scan (TENIS syndrome), defining a useful diagnostic protocol for re-staging and choosing the right treatment is inevitable. Numerous diagnostic modalities have been suggested in these cases. FDG PET / CT is a common scan used to reclassify differentiated thyroid cancer in patients with TENIS syndrome, but despite the positive findings, the diagnostic modality is still not effective. In recent years, new theranostics based on Y-90 and Lu-177 have been introduced, which can be labeled with various tracers, including somatostatin analogues, and also provide PRRT. On the other hand, in the differentiation of thyroid cancers, the thyroid cancer population may express different receptors, including somatostatin. The aim of this study was to investigate the role of F18-FDG PET / CT and Ga68-DOTATOC PET / CT in staging according to the diagnosis of local recurrence and metastasis, change of patient management and comparison of the results of these two modalities.

Methods & Materials: In this retrospective study, 20 patients with differentiated thyroid carcinoma were followed up in the thyroid clinic of the nuclear medicine ward of Ghaem Hospital in Mashhad. Patients with Tg values above 10 with TSH stimulation by levothyroxine withdrawal or Tg values above 5 on TSH suppression) following surgery, thyroid ablation or iodine therapy along with recent negative whole body scans with I-131 were evaluated in this study. All patients underwent F18-FDG PET / CT scan first and underwent Ga68-DOTATOC PET / CT scan for a maximum period of one week.

Results:20 patients with TENIS syndrome who had postablation iodine scans in 19 cases and diagnostic iodine scans in one case were examined, in which 50% of the study population were men (10 people). The primary pa-

thology of thyroid cancer was PTC in 19 patients and FTC in one case. 14 patients (70%) had classical subtype (four cases of follicular variant subtype) and 6 other patients had non-classic variants including diffuse sclerosing, Hurthle cell, Hurthle cell with oncocytic and poorly differentiated with insular variants. The total number of positive findings based on the location of the lesions in both scans was 23/27 and based on the patient in Ga-DOTATOC and FDG were 65% (13/20) and 70% (14/20), respectively. Stage of the disease in most patients according to the seventh edition was stage IV (12 patients) and based on the eighth edition (10 patients) was in stage I of the disease. All 13 patients with positive findings in Ga-DOTATOC were candidate for a treatment plan. Six patients were treated with Lu177-DOTATATE, five patients underwent surgery, one patient underwent surgery and radiotherapy, and one patient underwent simultaneous treatment with lutetium and radiation therapy. Of the 14 patients with positive FDG scans, 6 underwent surgery and one underwent simultaneous radiotherapy and surgery. The overall results of both modalities based on discontinuation of the pill or TSH suppression were not significantly different (p-value < 0.999). The statistical relationship between the number of positive and negative findings of patients in the two PET tracers was not significant (p = 1). Comparison of distribution of Tg levels in patients based on Ga-DOTATOC and FDG scan findings was not of significant relationship also no statistial significance was found between pathological subtypes (classical and non-classical types) as well as Tg levels and Ga-DOTATOC findings (p-value = 0.67). While there was a significant relationship between Tg levels and FDG findings (p-value = 0.015) there was no significant relationship between Tg levels and FDG positive findings in TSH stimulation state (p = 0.262). Also, there was no significant relationship between Tg levels and pathological subtypes (p-value = 0.602).

Conclusion: Expression of somatostatin receptors by Ga68-DOTATOC PET / CT uptake is observed in significant percentage of patients with elevated Tg level negative whole-body iodine scintigraphy. The positive findings of the two modalities are not significantly different and it seems that Ga-DOTATOC is involved in the treatment plan of patients who have a positive FDG PET / CT finding with no change in the management of the disease.

Keywords: Differentiated thyroid cancer, TENIS syndrome, F^{18}-FDG PET/CT, Ga^{68}-DOTATOC PET/CT

Oral Presentation Papers

99mTc-labeled HYNIC-MI-432, as Novel Peptidomimetic Inhibitor of TMPRSS2 in Prostate Adenocarcinoma Progression and Metastasis by Tumor Imaging

Objectives: This study aimed to prepare 99mTc-labeled HYNIC-MI-432 for TMPRSS2 protease-targeted prostate cancer diagnosis.
Materials and Methods: The formerly designed MI-432 as peptidomimetic inhibitor of TMPRSS2 was conjugated with HYNIC as a well-established chelator and then radiolabeled directly with 99mTc as an appropriate radiotracer using tricine/EDDA as an exchange coligands. Radiochemical purity, normal saline, and serum stability were evaluated by a radio-isotope TLC scanner and also confirmed by RP-HPLC. The cellular-specific binding of 99mTc-labeled HYNIC-MI-432 was assessed toward the prostate cancer cell line (PC3). Moreover, in-vivo investigations were carried out in PC3 xenograft tumour-bearing nude to trace the biodistribution of prepared radio-conjugate in various organs and the tumour site. Eventually, the 99mTc-labeled HYNIC-MI-432 was used for tumour imaging using planar SPECT.
Results: Radiolabelling was achieved with high purity and accompanied by a suitable shelflife. The cellular studies demonstrated the radio-conjugate specific binding in cultured PC3 cell line. In-vivo experiments showed rapid blood clearance of 99mTc-labeled HYNIC-MI- 432 with mainly renal excretion and tumour uptake specificity. SPECT imaging studies revealed a prominent accumulation of 99mTc-labeled HYNIC-MI- 432 in TMPRSS2-expressing PC3 tumours. The results of planar SPECT imaging also confirmed a considerable accumulation of 99mTclabeled HYNIC-MI-432 in TMPRSS2-expressing PC3 tumours.
Conclusion: TMPRSS2 is increasingly expressed in prostate cancer. This can be a suggestive route to detect prostate adenocarcinoma by SPECT imaging using radioligands that selectively interact with this protease.

Oral Presentation Papers

Evaluating the correlation of LV mechanical dyssynchrony by phase analysis of gated-SPECT MPI with QRS width in heart failure patients

Department of Nuclear Medicine, Namazi Hospital, School of Medicine, Shiraz University of Medical Sciences, Shiraz, Iran

Background: One of pathophysiologic mechanism that contributes to reduced LVEF in heart failure (HF) patients is dyssynchronous contraction of LV walls, which can be caused by abnormal electrical activation, reflected by prolonged QRS width on ECG. Although both electrical and mechanical dyssynchrony are common in patients with HF, mechanical dyssynchrony can be observed in these patients even without electrical dyssynchrony, whereas the main criteria for cardiac resynchronzation therapy (CRT) is based on ECG. The aim of the present study is to compare the prevalence of mechanical dyssynchrony, based on phase analysis of gated-SPECT MPI in HF patients with and without electrical dyssynchrony, based on QRS width.
Material and methods: This is a cross-sectional study conducted during 2 years on patients who were referred for SPECT MPI. The patients with EF<50% in gated-SPECT MPI were included. The patients were divided into two groups with QRS≥120 (wide QRS) or <120ms (narrow QRS) based on 12-lead ECG, obtained during SPECT-MPI. The LV dyssynchrony parameters including phase histogram bandwidth (PHB), phase standard deviation (PSD) and entropy were extracted from the phase analysis of QGS software and compared between the patients with and without electrical dyssynchrony.
Results: One hundred and twenty-nine patients were enrolled including 93 (73%) patients with narrow QRS. The mean value of PHB, PSD and entropy were 74.8±40.0, 21.7±10.8 and 55.7%±9.7 in wide-QRS group and 70.4±38.2, 19.3±10.5 and 51.7±11.0 in narrow-QRS group, respectively. The frequency of patients with mechanical dyssynchrony did not differ significantly between those with QRS>120ms and QRS<120ms, as well (38% in narrow-QRS and 41% in wide-QRS groups). There was also no statistically significant correlation of QRS width with PHB, PSd or entropy. The mean value of other functional parameters also showed no significant difference between these QRS-base groups.

Conclusion: According to the results of this study, a high percentage of electromechanical dissociation has been proposed in HF patients. Considering the greater relationship between mechanical dyssynchrony and other functional parameters, it is suggested to incorporate mechanical dyssynchrony indices in the workup of HF patients who are candidate for CRT.

Oral Presentation Papers

Evaluating the diagnostic value of whole-body ^{99m}Tc-HYNIC-PSMA 11 scan along with SPECT/CT imaging as a single modality for initial staging of intermediate to high-risk prostate cancer patients

Vahid Roshanravan[1], Atena Aghaee[1]*, Hamidreza Ghorbani[2], Salman Soltani[2], Behzad Aminzadeh[3], Reza Jafaei Dalouei[1], Kamran Aryana[1], Kayvan Sadri[1], and Hasan Mehrad-Majd[4]

1- Nuclear Medicine Research Center, Mashhad University of Medical Sciences, Mashhad, Khorasan Razavi, Iran
2- Kidney Transplantation Complication Research Center, Mashhad University of Medical Sciences, Mashhad, Iran
3- Department of Radiology, Faculty of Medicine, Mashhad University of Medical Sciences, Mashhad, Iran
4- Clinical Research Development Unit, Faculty of Medicine, Mashhad University of Medical Sciences, Mashhad, Iran

Background: In this prospective study, we aimed to compare the diagnostic yield of conventional imaging modalities – namely, CT scan, bone scan, and Tc-99m-HYNIC-PSMA 11 – in detecting local and distant metastases for the initial staging of intermediate to high-risk, treatment-naïve prostate cancer patients.

Material and Methods: A total of 63 treatment naïve PCa patients were enrolled in the study for initial staging. These patients underwent chest and abdominopelvic CT scans, bone scans, and Tc-99m-HYNIC-PSMA11 imaging. The Tc-99m-HYNIC-PSMA11 imaging was performed 3 to 4 hours post intravenous injection of 20-25 mCi Tc-99m-HYNIC-PSMA 11 and 20-25 mCi Tc-99m-MDP. The maximum interval between these scans was 30 days. Nuclear imaging was conducted for the whole body, incorporating either SPECT or SPECT/CT phases. These scans specifically focused on two main regions: the thorax and the abdominopelvis, with additional scans of any areas deemed suspicious. Images from each modality were independently interpreted, with analysis being either patient-based or region-based.

Results: In a patient-based analysis, osseous metastases detection rates for

the PSMA scan, CT, and bone scan were 31.7% (20/63), 34.9% (22/63), and 33.3% (21/63), respectively. There was no statistically significant difference among these modalities. For region-based analysis, metastatic osseous regions were identified in: PSMA scan, 78 regions (median: 0 areas per patient, range: 0-9), CT, 25 regions (Note: comprehensive evaluation of all 9 osseous regions was restricted due to the CT's limited field), and bone scan, 87 regions (median: 2 areas per patient, range: 0-9). The detection rates for local lymph node and distant metastases (including distant lymphatic, osseous, and visceral sites) were: PSMA scan: 28.6% (18/63) and 36.5% (23/63), respectively. CT scan: 31.8% (20/63) and 42.9% (27/63), respectively. There was no significant difference in these rates between the two modalities. Cumulatively, positive findings from the PSMA scan alone, CT scan alone, and combined PSMA and bone scans were observed in 49.2% (31/63), 53.9% (34/63), and 50.8% (32/63) of patients, respectively. Equivocal results were noted in 1 patient for the PSMA scan, 13 for the CT scan, and 4 for the bone scan. When considering these equivocal results as indicative of metastasis: PSMA scan exhibited a sensitivity of 60% and a specificity of 96.4%. CT scan demonstrated a sensitivity of 62.9% and a specificity of 89.3%, and bone scan reported a sensitivity of 78.6% and a specificity of 91.4%. While the CT scan identified patients with local and distant metastases more frequently, and the bone scan revealed more patients with distant bone metastasis compared to the PSMA scan, there were no statistically significant differences in overall staging or positivity rates between the modalities. Lastly, a substantial agreement was observed between the staging derived from the PSMA scan combined with the bone scan and that of the added CT scan (K values of 0.949 and 0.905, respectively, both $p < 0.001$).

Conclusion: The accuracy and concordance of 99mTc-HYNIC-PSMA 11, when used in conjunction with a CT scan and bone scan, demonstrate its viability as a reliable method for the initial staging of intermediate to high-risk prostate cancer patients.

Keywords: Tc-99m-HYNIC-PSMA11, CT scan, bone scan, initial staging, diagnostic value

Oral Presentation Papers

Selecting Stress-Only Patients in Myocardial Perfusion SPECT Imaging Based on Machine Learning

Mahshid Mortezanejad[1], Seyed Mohammad Entezarmahdi[1,2], Reza Faghihi[1], Tahereh Ghaedian[2], Fatemeh Abbasi[1]

1. Nuclear Engineering Department, Shiraz University, Shiraz, Iran
2. Department of Nuclear Medicine, School of Medicine, Shiraz University of Medical Sciences, Shiraz, Iran
Email: mahshidmrt@gmail.com
Tell: 09304769414

Introduction: Canceling rest scan in patients with normal stress scan will reduce the radiation dose received by patient and imaging time. For this purpose, in this project, we try to identify those patients for whom rest scan is not necessary by utilizing machine learning (ML) with quantitative scan parameters and patient demographic data.
Method: In this study, 120 patients with normal stress-rest cardiac SPECT and 120 patients with abnormal MPI SPECT were selected. The clinical quantitative parameters extracted from the Cedars QPS/QGS. Based on two models of Random Forest and Support Vector Machine, optimized features from stress image and demographic data were selected. By using 9 different decision machines and the selected features, the patients were categorized as normal and abnormal. Area under the Roc curve (AUS) and sensitivity of the proposed models were computed and compared with the decision of the nuclear medicine physician.
Results: The highest sensitivities obtained were 0.74 and 0.72 for the decision tree and the logistic regression machines, respectively. Also, the highest AUCs obtained were 0.88 and 0.87 for the Gaussian Naive Bayes and Logistic Regression machines, respectively. Compared to the physician's decision, which had Sensitivity and AUC of 0.89 and 0.7 respectively, the proposed machines have lower Sensitivity but better AUC.
Conclusion: Given the results obtained, machine learning can be used as an efficient tool to select stress-only patients in myocardial perfusion SPECT imaging.
Keywords: Stress-only protocol, Myocardial Perfusion SPECT, Machine Learning

Oral Presentation Papers

Preparation and evaluation of Technetium-99m Labeled Human Serum Albumin nanoparticles for tumor imaging

Zhila Fallah, Mostafa Erfani, Azadeh Mikaeili, Mostafa Goudarzi

Radiation Application Research School, Nuclear Science and Technology Research Institute (NSTRI), Tehran- 1439951113, Iran.

Imaging methods lead to detect cancer in the early stages, prevent its further progression and increase the probability of the patient's viability. So, development of new imaging methods has been considered in the medicine. Human serum albumin particles, which could be labelled with diagnostic and therapeutic radionuclides, are being introduced as carriers for radiopharmaceuticals. (1). The physical properties of ^{99m}Tc-labelled HSA-particles, including their size and shape, allow for a broad range of diagnostic applications. For example, ^{99m}Tc-HSA particles in the range of 10-100 µm use in the lung perfusion imaging. These type of particles in the range of 50-80 nm use as a diagnostic radiopharmaceutical for the sentinel lymph node scintigraphy (2-3).

In the present study, HSA-nanoparticles in the range of 50-100 nm were prepared using desolvation method. After purification and size-determination, HSA-nanoparticles were labeled with technetium-99m. Radiochemical purity and saline stability were determined by TLC method, and biodistribution studies were assessed in tumorized rats.

The size of the particles was found to be under 50 nm. Labeling yield was determined more than 98%. Stability evaluation of ^{99m}Tc-HSA-nanoparticles in saline solution indicated a radiochemical purity of over 90% within 4 hours. The biodistribution studies showed high tumor uptake with rapid kidney clearance. Imaging scintigraphy revealed that ^{99m}Tc-HSAnanoparticles were accumulated mainly in the tumor and kidneys as excretion pathway.

The results confirm that ^{99m}Tc-HSAnanoparticles could be a suitable imaging agent for tumor diagnosis.

Keywords: Albumin, Particles, Desolvation method, Technetium 99m

Oral Presentation Papers

New Radiolabeling of ^{99m}Tc for Hybrid Imaging-SPECT/MRI

Saleh Salehi Zahabi

1. Department of Radiology and Nuclear Medicine, Kermanshah University of medical sciences, Kermanshah, Iran.
2. Department of Medical physics, Lorestan University of medical sciences Lorestan, Iran.

Introduction: Iron oxide nanoparticles coated with chitosan can be detected as a contrast agent in MRI. If it is labeled with technetium, it can be a potential to prepare a new combined radiopharmaceutical for combined SPECT/MRI imaging.

Material and method: In this study, the shape and size of iron oxide nanoparticles coated with chitosan were investigated using SEM and DLS. After direct labeling with ^{99m}Tc, labeling efficiency and its stability were also checked. In the next step, this compound was injected into Balb\c mice and it was done at 30, 60, 90, 120 minutes after biological distribution. Finally, after the injection, MRI and nuclear medicine images were performed.

Result: The shape of the nanoparticles was spherical and the dimensions were in the range of 36-123 nm. Labeling efficiency was 93±4% and stability in phosphate buffer and blood serum was 94±3% and 97±2%, respectively. Biological distribution, nuclear medicine images and MRI also showed the high accumulation of this complex in the liver.

Conclusion: Considering the labeling efficiency and high stability of this complex and its high accumulation in nuclear medicine and MRI images in the liver, it can have the potential to be used as a combined SPECT/MRI radiopharmaceutical.

Keywords: ^{99m}Tc, SPECT/MRI, Nanoparticle, Radiolabeling

Oral Presentation Papers

A chemokine receptor targeted peptide labeled with ^{177}Lu as a new therapeutic agent

Mostafa Erfani[1*], Azadeh Mikaeili[1], Mostafa Goudarzi[1], Zhila Fallah[1], Mohammad Hasan Pejam[1], Maryam Mazaheri Tehrani[1],

1. Radiation Application Research School, Nuclear Science and Technology Research Institute, Tehran, Iran.

Aim/Introduction: Chemokine receptors belong to the wide family of G-proteins coupled seven transmembrane domain receptors which are expressed in cell surface. There is one chemokine receptor that is known to be up-regulated in many types of tumor cells, namely CXCR4. Thus, CXCR4 receptors could be employed for tumor imaging and therapy.
Materials and Methods: A CXCR4 targeted peptide was designed and prepared after labeling with ^{177}Lu. Afterward, cell uptake, receptor binding, internalization, in vivo tumor uptake and biodistribution were assessed. The receptor binding and internalization rate were evaluated using C6 glioma tumor cells. Rats bearing C6 tumors were employed for investigation of radiotracer biodistribution and imaging.
Results: Radiotracer was prepared with labeling yield and radiochemical purity of >90%. Stability up to 24 hours was confirmed by incubation of radiotracer in human serum at 37°C and analysis with HPLC. The in vitro cell uptake test resulted specific uptake of radiotracer in C6 glioma tumor cells. TIn receptor binding study Kd = 155.1 ± 10.14 nM was obtained for radiotracer. The in vivo biodistribution parameters were studied in the rat after intravenous injection of radiolabeled [^{177}Lu]Lu-CXCR4. ^{177}Lu-labeled CXCR4 was mainly taken up by the kidneys and liver which was very different from those of other organs. Animal biodistribution data showed tumor uptake after 1-hour post administration. Gamma imaging study demonstrated that radiotracer was mainly accumulated in the tumor and kidney with a fast blood clearance which further confirmed tumor and kidney uptakes.
Conclusion: Our results indicate that this radiotracer has excellent capacity to accumulate in tumor in rat and to be included as a radiopharmaceutical for treatment of cancer tumors. Our findings demonstrated that the radiotracer can be a suitable candidate for glioma tumors targeting and treatment.

Oral Presentation Papers

Comparing diagnostic value of addition of SPECT and SPECT/CT to Whole Body I-131 scan (WBS) in differentiated thyroid cancer patients.

Hadis Mohammadzadeh Kosari[1], Seyed Rasoul Zakavi[2], Atena Aghaei[2], Somayeh Barashki[2], Donia Hemmati[2], Susan Shafiei[2]

1. Nuclear Medicine Department, Imam Hossein hospital, shahroud University of Medical Sciences, shahroud, Iran
2. Nuclear Medicine Research Center, School of Medicine, Mashhad University of Medical Sciences, Mashhad, Iran

Objective: The purpose of this single-center prospective study is to compare the diagnostic value of addition of SPECT and SPECT/CT acquisition to planar post-ablation whole body iodine scintigraphy.
Methods and Materials: The study included 214 patients (145 women and 69 men) with an average age of 42.9 ± 14.9, who were referred for radioactive iodine treatment. Two hundred patients had papillary thyroid cancer (PTC) and 14 patients had follicular thyroid cancer (FTC). All patients underwent whole body iodine scans, followed by SPECT and SPECT/CT acquisition of the neck, chest, and any suspected regions. Three sets of images were reviewed and reported separately by an experienced nuclear physician.
Results: N classification was changed using SPECT/CT in 44 patients (20.6%) compared to planar images and in 42 patients (19.6%) compared to SPECT images as planar and SPECT images revealed new lymphatic metastases on dedicated SPECT/CT views in 17 and 22 patients, respectively. SPECT/CT images also changed M classification in 13 patients (6.1%) compared to planar images and in 16 patients (7.5%) compared to SPECT data. Adding SPECT/CT to planar images resulted in significant change in management and N or M staging among patients with multiple cycles of RAI compared to first cycle of RAI (P<0.001 & P= 0.01), significant change in management among patients who had Tg levels of ≥33 compared to lower Tg levels or those who received RAI more than 30 mCi compared to 30 mCi I-131 administration (P= 0.001 & P=

0.01, respectively), as well as comparable change in N/M staging among the latter (P= 0.056).

Conclusion: Based on the results of this study, it seems that addition of SPECT/CT had a significant impact on the management and classification of N/M in high-risk patients or patients with high Tg levels (above 33 ng/ml), those who received higher accumulative iodine dose (more than 30 mCi) and those with history of multiple doses of radio-iodine. In addition, the study concluded that when SPECT/CT is not available, performing SPECT alone is not recommended as it provides very little additional information and may even mislead the physician in some cases.

Keywords: SPECT/CT, SPECT, iodine-131, whole-body scan, differentiated thyroid cancer

Oral Presentation Papers

Comparison of ^{99m}Tc-HYNIC-PSMA-11 and Bone Scan in Detection of Bone Metastases in mCRPC patients: a single center experience

Somaye Barashki[1], Atena Aghaee[1]; Kamran Aryana[1]

1. Nuclear Medicine Research Center, Mashhad University of Medical Science, Mashhad, Iran

Background: Prostate-Specific Membrane Antigen (PSMA) is overexpressed in primary and metastatic prostate cancer (PCa) tissues. While PSMA PET agents have gained their role in the prostate cancer guidelines, Technetium-based PSMA agents have left behind. We compared ^{99m}Tc-HYNIC-PSMA-11 scan with bone scan and post treatment scan to evaluate the expression of PSMA in bone metastases, and confirm PSMA uptake in metastatic castration-resistant prostate cancer (mCRPC) patients before ^{177}Lu-PSMA therapy.

Methods: Thirty-nine mCRPC patients were included in the study. Bone and PSMA scans with a maximum interval of 90 days were performed 3-4 hours after intravenous injection of 20-25 mCi of ^{99m}Tc-MDP, and 15-25 mCi of ^{99m}Tc-HYNIC-PSMA-11, respectively. If the PSMA scan was positive, patients were treated with ^{177}Lu-PSMA and 24-48 hours after treatment a whole-body scan was obtained. For negative PSMA results, ^{68}Ga-PSMA PET/CT was performed to compare its results with the bone scan. In patients with PSMA expression, detection of metastatic lesions in two consecutive whole-body scans (^{99m}Tc-MDP and ^{99m}Tc-PSMA) in different regions were compared.

Results: The mean age of participants was 69.7 ± 9.3 (range: 51-87). All patients had prior evidence of bone metastases while 37 (94.9%) showed adequate ^{99m}Tc-PSMA uptake in the metastatic regions. The comparative sensitivity of the ^{99m}Tc-PSMA scan was calculated as 94.8%. Compared to bone scan, ^{99m}Tc-PSMA showed additional lesions in 13 (35.1%) participants. These additional lesions were mostly located in the appendicular skeleton and pelvic bones, especially iliac bones. Inversely, the bone scan detected more lesions in 12 (32.4%) patients; most of these additional lesions were in the ribs. Both scans in 12 (32.4%) patients showed the exact

same results. Comparison between the ^{99m}Tc-PSMA scan and ^{177}Lu-PSMA showed completely similar results in 29 (78.4%) patients; ^{177}Lu-PSMA detected more lesions in eight (21.6%) participants.

Conclusion: The ^{99m}Tc-HYNIC-PSMA scan showed mostly equivalent results to the bone scan in mCRPC patients. It is a low-cost modality for predicting suitable patients for radioligand therapy, especially in resource-limited countries.

Keywords: PSMA; SPECT/CT; ^{99m}Tc-; prostate cancer; bone scan; radioligand therapy

Oral Presentation Papers

Characterization of geometrical indices of gated-SPECT MPI in ESRD patients

Tahereh Ghaedian[1], Zeinab Azarnew[2], Abdolmajid Alipour[1], Sadegh Ebrahimi[1]

1. Department of Nuclear Medicine, Namazi Hospital, School of Medicine, Shiraz University of Medical Sciences, Shiraz, Iran
2. Student Research Committee, School of Medicine, Shiraz University of Medical Sciences, Shiraz, Iran

Introduction: In addition to coronary artery disease (CAD) as a cause of ischemic cardiomyopathy, the incidence of non-ischemic cardiomyopathy and heart failure is also higher in end-stage renal disease (ESRD). Imaging studies revealed that geometrical and structural changes are the preceding findings in ESRD patients with heart failure. Shape and eccentricity indices derived by gated-SPECT MPI have also been suggested to be correlated with heart failure in different patient groups. However, the value of these different parameters has not been precisely assessed in ESRD patients.
Methods: In this cross-sectional study, all ESRD patients who were referred for stress-rest SPECT MPI during one-year period and those with normal myocardial perfusion in gated-SPECT MPI were included. The quantitative LV geometric parameters include shape index (SI) and eccentricity index (EI) in stress (SI-S and EI-S) and rest (SI-R and EI-R) perfusion scan and SI and EI at end-diastole (ED_SI, ED-EI)) and end-systole (ES-SI, ED-ES-EI) frame of gated study. Based on EF, patients were divided into two groups with EF below and above the 50%. The correlation of geometric parameters with different LV functional parameters were evaluated and the mean values of all parameters were compared between the two EF group.
Results: In this study, 160 ESRD patients with normal perfusion on SPECT MPI were enrolled. The average age of patients was 51.89 ± 1.04 with female/male ratio of 64/96. In comparison of ESRD patients with EF≥50% (N=132) and those with EF<50% (N=28), the SI indices were all significantly higher in low EF group, but EIs showed no significant difference. SI-ES had the greatest significant correlation coefficient with EF (r: -0.630, P<0.001). Since all patients with reduced EF had EDV>120 ml, a subgroup

of patients with normal EF but EDV>120 ml (n=40) were also selected and compared with low-EF group. While SI-ES, PFR and MFR/3 were remained significantly different between these groups, other diastolic and dyssynchrony indices were not statistically different.

Conclusion: SI_ES is a more robust and relevant functional index as compared to other LV geometrical parameters and can serve as a functional discriminative parameter in ESRD patients. SI-ES had the greatest correlation with EF as compared to other diastolic and dyssynchrony parameters in ESRD patients. Further prognostic and dedicated study for the evaluation of SI-ES, especially in the early detection of non-ischemic heart failure in ESRD patients and validation of the optimal cut-off value are recommended.

Keywords: Heart failure, ESRD, SPECT MPI, shape index

Oral Presentation Papers

How necessary it is to perform a ventilation scan in patients with a history of COVID-19 to rule out PTE?

Farivash Karamian[1], Roham Nikkhah[2], Mohammad Ghorbani[3], Elham Rahmanipour[4], Mohammad Mohammadi[5], Emran Askari[6], Ramin Sadeghi[7*]

1. Resident of nuclear medicine, Nuclear Medicine Research Center, Mashhad University of Medical Sciences, Mashhad, Iran
2. Isfahan Medical Students Research Committee (MSRC), Isfahan University of Medical Sciences, Isfahan, Iran
3. Medical student, Faculty of Medicine, Mashhad University of Medical Sciences, Mashhad, Iran
4. Medical student, Faculty of Medicine, Mashhad University of Medical Sciences, Mashhad, Iran
5. School of Medicine, Iran University of Medical Sciences, Tehran, Iran
6. Assistant Professor of Nuclear Medicine, Department of Nuclear Medicine, School of Medicine, Nuclear Medicine Research Center, Ghaem Hospital, Mashhad University of Medical Sciences, Mashhad, Iran
7. Associate Professor of Nuclear Medicine, Department of Nuclear Medicine, School of Medicine, Nuclear Medicine Research Center, Ghaem Hospital, Mashhad University of Medical Sciences, Mashhad, Iran

Introduction: This study aimed to assess the feasibility of a method and determine the necessity of ventilation scans in patients with a history of COVID-19 infection suspected of having pulmonary embolism (PE). Additionally, the study aimed to report practices and imaging findings in this specific population.

Method: A cross-sectional study was conducted at a tertiary care hospital in 2020, involving patients with PCR-confirmed COVID-19 and suspected PE. VQ scintigraphy using SPECT/CT and CT scans with or without contrast were performed. Blinded nuclear medicine physicians interpreted the images for PE and COVID-19, while clinical and laboratory data were analyzed.

Result: Out of 96 patients with suspected PE and COVID-19 infection, eight patients unable to undergo ventilation scans were excluded. Among

the remaining patients, five had multiple mismatched ventilation/perfusion (V/Q) defects on SPECT/CT, confirming PE. PE was ruled out in 83 patients who had either normal perfusion scans, perfusion defects with COVID-19 features, or matched V/Q defects. The study found a prevalence of PE at 5.68% and determined that ventilation scans were necessary for 28.4% of the patients in this population.

Conclusion: In conclusion, lung scintigraphy was effective in diagnosing pulmonary embolism in COVID-19 patients, with a 5.68% prevalence rate and a 28.4% requirement for ventilation scans.

Keywords: SPECT/CT scan, COVID-19, pulmonary embolism, ventilation scan.

Oral Presentation Papers

Accuracy of sentinel node mapping in Marjolin ulcer: comparison of three different injection techniques

Pegah Sahafi; Ehsan Soltani; Ehsan Hasanzadeh Haddad; Ezzatollah Rezaei; Nema Mohamadian Roshan; Vahid Reza Dabbagh; Ramin Sadeghi

Background: Marjolin ulcer is a specific type of squamous cell cancer that can benefit from the use of lymphoscintigraphy.The purpose of this study was to evaluate 3 different injection techniques for sentinel node biopsy in patients with Marjolin ulcer.
Methods: Forty-eight patients with Marjolin ulcer (27 male and 21 female) ranging in age from 24-85 years were included in our study. Intratumoral (IT), peritumoral (PT) and periscar (PS) tissue injections of radiotracer were done in 9, 10, and 29 patients respectively. Injections were done 2-4 hours before surgery. Lymphoscintigraphy was done for mapping the lymphatic drainage. During surgery, lymphatic mapping and sentinel node biopsy was performed using a handheld gamma probe. After harvesting sentinel nodes, regional lymph node dissection was done.
Result: Sentinel node detection rate was higher in the PS group as compared to the IT and PT groups (89.6% vs. 50% and 22.2%) respectively. False negative rate was 0%.
Conclusion: Lymphatic mapping and sentinel node biopsy is feasible in Marjolin ulcer with high detection rate and low false negative cases. Injection site is the main factor influencing the success of the procedure and injection of the mapping material in the peri-scar normal skin proximal to the lesion is the best technique.

Oral Presentation Papers

Evaluating the salivary gland function indexes by Tc99m salivary scan, after partial parotidectomy

Atena Aghaee

Objective: Parotid pleomorphic adenomas necessitate surgical intervention, with a growing emphasis on preserving salivary function post-surgery due to its critical role in maintaining oral health and overall quality of life. This study aims to evaluate a surgical method meticulously designed to preserve salivary function following partial superficial parotidectomy, utilizing Technetium-99m scintigraphy.

Methods & Materials: This single-center prospective cohort study was conducted in Mashhad, Iran, between 2022-2023. The study encompassed 40 patients diagnosed with parotid pleomorphic adenomas, with an age range of 20 to 64 years, undergoing partial superficial parotidectomy. Salivary function was evaluated using Technetium-99m scintigraphy three weeks post-operation. Data were analyzed using SPSS statistical software (version 26), employing descriptive statistics and Wilcoxon rank sum tests for statistical analysis.

Results: The cohort predominantly consisted of individuals who underwent right parotid surgery (62.5%) compared to left parotid surgery (37.5%). The study revealed that the partial superficial parotidectomy is generally effective in maintaining saliva secretion on the operated side, with no reported complications within the three-week post-operative period. The procedure also demonstrated a good safety profile.

Conclusion: In conclusion, our study demonstrated that the superficial parotidectomy technique, when focused on preserving the salivary function of the deep parotid gland, is notably effective. Not only does it maintain saliva secretion on the operated side, but it also boasts an admirable safety profile. There were no recorded complications, and the preservation of the duct was achieved in a vast majority of the instances.

Oral Presentation Papers

Effects of radioactive iodine therapy on female sex hormones and menstrual cycle in patients with thyroid carcinoma

Atena Aghaee[1]; Amirhossein Akhavan-Mahdavi[2*], Mohammadhossein Yekta[2], Susan shafiei[1]; Somayeh Moein Darbari[3]; Seyed Rasoul Zakavi[1], Maryam Emadzadeh[4], Emran Askari[1], Yasaman Fakhar[1], Hadis Mohammadzadeh Kosari [1]

1. Nuclear medicine research center, Mashhad University of Medical sciences, Mashhad, Iran.
2. Faculty of medicine, Mashhad University of Medical Sciences, Mashhad, Iran
3. Department of Obstetrics and Gynecology, Neonatal and Maternal Research Center, Mashhad University of Medical Sciences, Mashhad, Iran
4. Clinical Research Unit, Faculty of Medicine, Mashhad University of Medical Sciences, Mashhad, Iran

Background: Differentiated thyroid carcinoma (DTC) is the most common endocrine malignancy. Total thyroidectomy with subsequent radioactive iodine therapy (RIT) followed by levothyroxine consumption is a routine approach to deal with DTC. Widespread use of RIT in patients with DTC has raised concerns about its potential adverse effects on female reproductive organs. We aimed to check the effects of postoperative RIT on menstrual symptoms and sex hormones in patients with DTC.

Methods: Women in reproductive age with DTC admitted in Nuclear Medicine department from 2020 to 2021 were studied. The demographic and menstrual information was recorded at first presentation and follow-up visits. Blood samples were taken for measurement of follicle stimulating hormone (FSH), luteinizing hormone (LH), anti-Müllerian hormone (AMH), and estradiol at baseline, 6 and 12 months after RIT. ……...

Results: 77 women with DTC and mean age of 35 years were studied. Roughly half (50.4%) received high-dose RIT (i.e. ≥100 mCi administered radioiodine). No patient had distant metastasis. Dysmenorrhea was reported in 23 (29.9%) of the patients and flushing was seen in 6 (7.8%). The number of pads used during menstrual periods, the length of menstrual periods

and its frequency decreased significantly 2 months after RIT and returned to baseline values one year after RIT. The LH, FSH, and estradiol levels has increased continuously 6 and 12 months after RIT. In contrast, the mean serum level of AMH was not changed compared to that of the pre-treatment level. The changes in sex hormones and menstrual cycles were not different between the low and high-dose RIT groups ($p > 0.1$).

Conclusion: The serum levels of LH, FSH, and estradiol hormones increased after RIT for up to 12 months after RIT while the AMH levels were stable. The menstruations were adversely affected 2 months after radioactive iodine therapy regardless of the dose of radio-iodine and improved by 6 months.

Keywords: Thyroid cancer, Menstrual cycle, Radioactive iodine, sex hormones

Oral Presentation Papers

Quantitative Evaluation of Effective Parameters in FDG-PET Imaging of Tumor-Bearing Mice: Impact of Fasting Durations, Anesthetic Agents, and Darkness

Kaveh Tanha[1,2], Mohammad Seyedabadi[3,4], Hossein Ghadiri[1,2], Mohammadreza Ay[1,2]

1. Department of Medical Physics and Biomedical Engineering, Tehran University of Medical Sciences, Tehran, Iran
2. Research Center for Molecular and Cellular Imaging, Tehran University of Medical Sciences, Tehran, Iran
3. Department of Toxicology and Pharmacology, Faculty of Pharmacy, Mazandaran University of Medical Sciences, Sari, Iran
4. Pharmaceutical Sciences Research Center, Faculty of Pharmacy, Mazandaran University of Medical Sciences, Sari, Iran

Introduction: Positron emission tomography (PET) using [18F]Fluorodeoxyglucose (FDG) is a crucial tool for studying tumors in small animals. To attain reliable and precise results in preclinical FDG-PET imaging, it is necessary to thoroughly evaluate and optimize various parameters. This study focused on evaluating the effects of fasting durations, anesthetic agents, and darkness on the outcomes of FDG-PET imaging in 4T1 tumor-bearing mice.

Materials and methods: Female BALB/c mice with 4T1 cell xenografts were used to study the impact of various parameters on FDG-PET scan results. A dose of 12 MBq FDG was injected, and imaging was performed 60 minutes post-injection of the radionuclide. The mean standardized uptake value (SUVmean), tissue-to-muscle ratios, and tumor-to-brain ratios were calculated for different tissues, and biodistribution studies were conducted by measuring the percentage of the injected dose per gram (%ID/gr) of tissues.

Results: Fasting caused a decrease in the SUVmean of the heart and muscle tissues. Additionally, it resulted in an increase in the tumor-to-muscle ratio, indicating a higher uptake of FDG in the tumor compared to the muscle tissue. The tumor exhibited the highest %ID/gr when a fasting duration of

3 hours was implemented. Isoflurane anesthesia led to a decrease in brain SUVmean and a significant reduction in brain FDG uptake. Ketamine/xylazine anesthesia resulted in decreased SUVmean for the tumor and muscle tissues. During ketamine/xylazine anesthesia, darkness decreased heart SUVmean but increased tumor-to-muscle and brain-to-muscle ratios. Surprisingly, in both ketamine/xylazine and isoflurane anesthesia conditions, darkness significantly increased %ID/gr within the tumor. Furthermore, under isoflurane anesthesia, darkness exhibited a similar effect by increasing %ID/gr in the brain, heart, and liver.

Conclusion: The results of this study indicated that a fasting duration of 3 hours would yield an appropriate tumor contrast in FDG-PET imaging. Different fasting durations affected tumor and brain SUVmean differently. Anesthesia and lighting conditions had notable effects on SUVmean and %ID/gr in various organs. Therefore, careful consideration of anesthetics, fasting duration, and ambient light is crucial for small animal PET imaging with FDG to ensure reliable and valid study results.

Keywords: ^{18}F-FDG, PET, Mice, Tumor, Fasting, Anesthesia

Oral Presentation Papers

Factors predicting the early biochemical response to [177Lu]Lu-PSMA therapy in patients with metastatic castration resistant prostate cancer

Ahmed Al-Timimi[1] , Reyhaneh Manafi-Farid[1], Babak Fallahi[1], Davood Beiki[1], Emran Askari[2] , Alireza Rezaei [3] , Zohreh Adinehpour[3] , Mohammad Eftekhari[1]

1. Research Center for Nuclear Medicine, Tehran University of Medical Sciences, Tehran, Iran
2. Nuclear Medicine Research Center, Mashhad University of Medical Sciences, Mashhad, Iran
3. Khatam PET/CT Center, Khatam Al-Anbia Hospital, Tehran, Iran

Introduction: Targeted radionuclide therapy with [177Lu]Lu-prostate-specific membrane antigen (PSMA) has shown promising results for the treatment of castration-resistant prostate cancer (mCRPC). Nevertheless, a proportion of patients do not respond to this therapy. Here, we aimed to evaluate the prognostic significance of the pretreatment pathologic and laboratory factors for the prediction of biochemical response to the first cycle of [177Lu]Lu-PSMA therapy.

Methods: In this retrospective study, mCRPC patients, referred for [177Lu]Lu-PSMA therapy, were included. We retrieved the data of patients, undergone [177Lu]Lu-PSMA, from March 2019 to March 2021. Multiple baseline pathologic and laboratory parameters were extracted and correlated with the response to the first cycle. The prostate-specific antigen (PSA) level was evaluated six weeks after [177Lu]Lu-PSMA therapy for the biochemical response.

Results: Forty-three patients with a mean age of 69.8±10.2 were included. Bone and visceral metastases were present in 81.4% and 14.0% of the patients, respectively. Except for two, all patients had received hormone- and chemotherapy. The mean PSA level was 189.9±259.0 at baseline. Following one cycle of [177Lu]Lu-PSMA, "≥ 10% PSA response" and "≥ 50% PSA response" were seen in 81.4% and 44.2% of the patients, respectively. Patients with higher baseline PSA more frequently had ≥ 10% PSA response (p= 0.004). Also, the reduction in the PSA level correlated with baseline PSA (p=0.013, r=0.375).

Conclusion: [177Lu]Lu-PSMA therapy results in the biochemical response in a considerable number of patients after one cycle. In nearly half of patients, PSA declines more than 50%. Higher baseline PSA is correlated with the level of PSA response. Keywords: Castration-resistant prostate cancer; [177Lu]Lu-PSMA; Radioligand therapy; Biochemical response